Binding energy of the metastable He^- ion

P. Kristensen, U. V. Pedersen, V. V. Petrunin, and T. Andersen
Institute of Physics and Astronomy, University of Aarhus, DK-8000 Aarhus C, Denmark

K. T. Chung
Department of Physics, North Carolina State University, Raleigh, North Carolina 27695

(Received 4 September 1996)

This paper presents theoretical *ab initio* calculations and experimental measurements of the binding energy of the metastable $He^-1s2s2p\ ^4P$ ion. The calculated 77.518 ± 0.011 meV and the measured 77.516 ± 0.006 meV values for the binding energy are in excellent agreement and they represent a significant improvement in the accuracy compared to previous studies. The experimental technique is based on the determination of the ϵs-wave Wigner threshold associated with detachment to the $1s3s\ ^3S$ state of the neutral He atom. The yield of the $1s3s\ ^3S$ He level was monitored by applying resonant ionization spectroscopy. [S1050-2947(97)00602-1]

PACS number(s): 32.10.Hq, 32.80.Gc

I. INTRODUCTION

Electron-electron correlation plays a dominant role in the understanding of the structure and dynamics of negative ions, since the binding energy in these systems often is smaller than or comparable with the correlation energy. Hence these systems provide an excellent opportunity for testing the ability of various theoretical models to incorporate correlation by comparing the predictions with experimental values obtained for the position and the width of resonances, binding energies, and lifetimes of stable and metastable states. In recent years, there has been a rapid development in the knowledge about the affinity of the lighter elements. The electron affinities of H [1] and O [2] have been known experimentally with a high accuracy for some time from coaxial-laser-detachment spectroscopy studies. Quite recently, the electron affinities of Li [3] and Be [4,5] were determined experimentally with only a few tens of μeV uncertainty, utilizing a combination of laser photodetachment and resonant-ionization spectroscopy.

For more than 20 years, the electron affinity (EA) of hydrogen has been known with a high accuracy from elaborate *ab initio* calculations by Pekeris [6,7] and Aashamar [8]. Although the two calculations differ by 0.06 cm^{-1}, it has not yet been possible to obtain experimental data [1] with sufficiently high accuracy to clarify this discrepancy. Very recently accurate *ab initio* calculations of the EA's of the Be atom have become available [9], deviating less than 0.3% from the experimental values [4,5]. In light of this very positive development, it also appears to be of interest to obtain even more accurate experimental values for He, the second-lightest element in the Periodic Table.

He^- exists in a metastable $1s2s2p\ ^4P$ state located approximately 0.08 eV below the parent He $1s2s\ ^3S$ state. The lifetime of the $1s2s2p\ ^4P_{5/2}$ state ($\tau_{5/2}=350\ \mu$s [10]) is more than one order of magnitude longer than for the $1s2s2p\ ^4P_{1/2,3/2}$ states ($\tau_{1/2}=16\ \mu$s and $\tau_{1/2}=10\ \mu$s [11]). According to Brage and Froese Fischer [12], all the ^4P_J levels decay primarily via two-body relativistic corrections, i.e., autodetachment by spin-spin and spin-other-orbit interactions. The $J=1/2$ and $J=3/2$ levels can decay to the $1s^2\ ^1S$ state by emitting an ϵp wave, whereas the $J=5/2$ level can decay only by emitting an ϵf wave yielding a much lower decay rate [12]. The $He^-\ 1s2s2p\ ^4P$ ion is sufficiently long lived to allow experimental studies of the ion to be performed, as it was done in the elegant experiments by Mader and Novick [13], who determined the fine-structure splittings of the $He^-\ 1s2s2p\ ^4P$ manifold with high accuracy by using a rf resonance technique and exploiting the different decay rates of the fine-structure levels.

An experimental determination of the binding energy of the $He^-\ 1s2s2p\ ^4P$ is, however, associated with some difficulties. With a binding energy of only ≈0.08 eV with respect to the He $1s2s\ ^3S$ state, it is not possible with standard laser technique to measure the threshold for this channel. The ϵp Wigner threshold resulting from detachment to the He $1s2p\ ^3P$ state has previously been investigated experimentally by Peterson and collaborators [14,15]. A determination of the threshold for detachment is inherently difficult due to the smooth behavior of the cross section for an ϵp wave. A further complication for this particular detachment channel is the large $He^-\ 1s2p^2\ ^4P^e$ shape resonance situated only 10.80 ± 0.07 meV above the threshold, with a width of 7.16 ± 0.07 meV [15]. An analytical expression for the cross section was derived from a careful analysis of the effect of a resonance close to a threshold for detachment. An impressive fit to the experimental data in a large region above the threshold made it possible to obtain not only the width and position of the $He^-\ 1s2p^2\ ^4P^e$ shape resonance, but also a value for the threshold energy yielding an EA of 77.67 ± 0.12 meV for He $1s2s\ ^3S$. However, the experimentally obtained value appears to be in slight disagreement with the best theoretical value [16].

Before 1996, the most accurate theoretical calculation of the energy of $He^-\ 1s2s2p\ ^4P^o$ was given by Bunge and Bunge [16], who used a 1000-term configuration-interaction

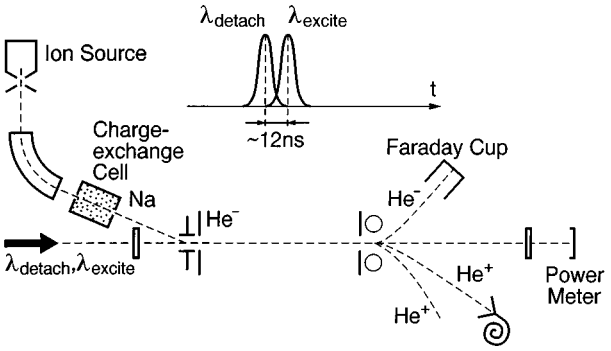

FIG. 1. Illustration of the experimental setup.

(CI) wave function to calculate the binding energy to be 77.51 ± 0.04 meV. Of the quoted uncertainty 0.01 meV came from the QED effect. In 1988, Drake [17] calculated the QED contribution to the ionization potential of helium. This also allows us to give a much better estimate for the QED contribution to electron affinity. In addition, Chung and Zhu [18] have recently developed a restricted variation method that can be used to extrapolate the energy with a much smaller uncertainty than the 0.03 eV given by Bunge and Bunge [16]. This recent development allows us to estimate the binding energy with higher accuracy by combining the more accurate estimate of the QED contribution with the accurate energy extrapolation method of Chung and Zhu [18].

The aim of the present investigation is to provide more accurate experimental and theoretical values for the EA of He $1s2s\ ^3S$, clarifying the discrepancy between theory and experiment and thereby also stimulating further development of the understanding of the properties of the lighter atomic negative ions.

II. EXPERIMENTAL SETUP

The experiment was performed with a collinear setup as shown in Fig. 1. Positive He ions are produced in a plasma-ion source, extracted and accelerated though 40 kV, and subsequently mass- and charge-state analyzed in a magnetic field. The He^+ beam is charge exchanged by double-electron capture in a Na vapor produced by heating a small container with bulk Na metal to 280 °C. Following charge-state analysis by electrostatic deflection, the negative-ion beam is coaxially overlapped with two nanosecond dye laser beams in a 100-cm-long interaction region defined by 3.5-mm apertures. The current of $He^- \approx 1$ nA is measured with a Faraday cup after the interaction region. The metastable He^- $1s2s2p\ ^4P$ ions are detached by the first laser $\lambda_{detach} \approx 415$ nm, leaving the neutral He atom in either the $1s2s\ ^3S$, the $1s2p\ ^3P$, or the $1s3s\ ^3S$ state. The second laser $\lambda_{excite} \approx 682.31$ nm, applied approximately 12 ns after the first, resonantly excites the atoms left in the $1s3s\ ^3S$ state to the $1s14p\ ^3P$ Rydberg state, which is subsequently selectively detected (see Fig. 2). The selective detection of Rydberg atoms formed in the interaction region exploits the fact that different Rydberg levels ionize at different electric-field strengths (different positions) in the nonuniform field of a field ionizer positioned at the exit of the interaction region. The field ionizer consists of two cylinders with a diameter of

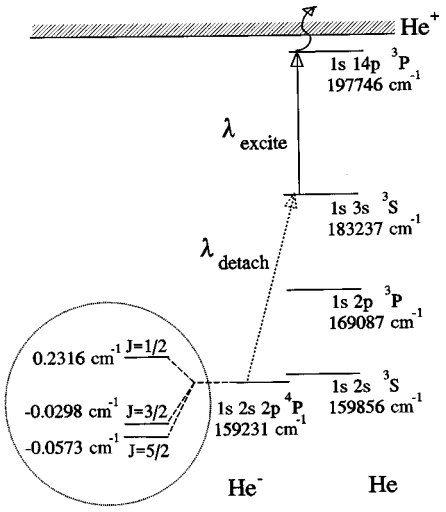

FIG. 2. Schematic energy-level diagram of He^- and He, indicating the studied detachment and excitation channel.

8 mm, separated by 12 mm, with a voltage of ≈12 kV across. Depending on the position at which the Rydberg atoms are ionized, the resulting positive ions are deflected into different angles. The population of a specific He Rydberg level is then selectively detected by measuring the resulting positive ions with an open electron multiplier placed 26 cm after the cylindrical ionizer at an angle of 12°. The mechanism of ionization of fast He Rydberg atoms in a similar setup has been investigated previously [19]. The number of positive ions produced after each laser shot is counted in a 600-ns time window by a SR400 Standford gated photon counter and accumulated in a personal computer as a function of the wavelength of the laser λ_{detach}. The 600-ns time window corresponds to the flight time though the field-free interaction region. The vacuum in the interaction region is kept below 10^{-7} torr to minimize the collisionally induced signal. The laser beam λ_{detach} used to detach the He^- is generated by a Lambda Physik Scanmate-2 dye laser, operated with stilbene 420 (10 mJ/pulse) and pumped by the 355-nm output of a 8-ns Nd:YAG laser (where YAG denotes yttrium aluminum garnet) with a repetition rate of 10 Hz. The second laser beam λ_{excite}, which is used to drive the resonant excitation from the He $1s3s\ ^3S$ level to the He $1s14p$ Rydberg level, is generated by a home-built dye laser operated with LDS 698 (5 mJ/pulse) and pumped by the 532-nm output of the same Nd:YAG laser.

In order to calibrate the wavelength scale of laser λ_{detach}, a small fraction of the laser beam is directed onto an optogalvanic argon lamp and two independent Fabry-Pérot interferometers. The signals from the interferometers and the optogalvanic lamp were recorded simultaneously with the positive-ion signal. The two interferometers have different spacings ($d_1 = 1$ cm and $d_2 = 0.6$ cm) between the high-reflective dielectric mirrors and serve as wavelength markers in the scans of the dye laser λ_{detach}. The optogalvanic lamp allows an absolute calibration of the interferometers by observation of different lines corresponding to transitions in Ar [20] (14 different lines in the vicinity of the observed threshold have been used). Due to the high finesse of the interferometers, the width of the fringes directly reflects the band-

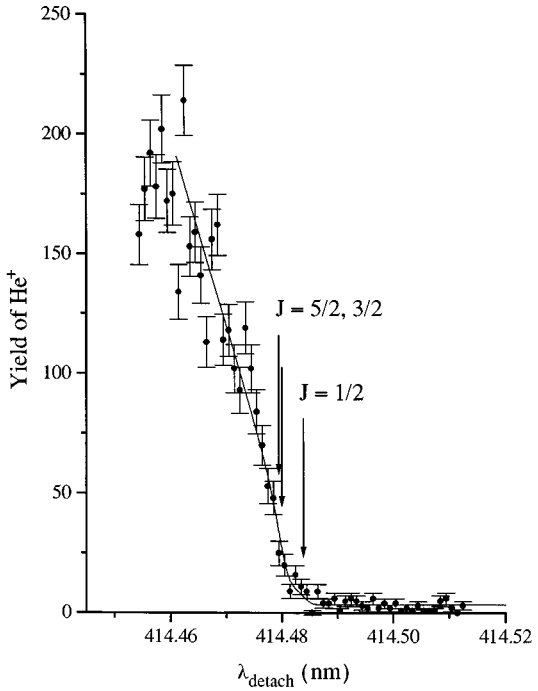

FIG. 3. Number of positive ions vs wavelength in air. The solid line indicates the best fit using Eq. (3.2). The three arrows indicate the position of the three thresholds $J=1/2,3/2,5/2$. The signal in each channel (0.001 nm) was obtained using 240 laser shots.

width of the laser $\Gamma \approx 0.11\ \mathrm{cm}^{-1}$ (full width at half maximum).

III. DATA AND ANALYSIS

The positive-ion signal vs wavelength at the opening of a new detachment channel is presented in Fig. 3. The signal corresponds to the sum of several scans obtained with the laser beam copropagating the ion beam. From Fig. 3 it is possible to observe the threshold for opening of the He^- $1s2s2p\ ^4P_{1/2}$ detachment channel at 414.484 nm. It is, however, not possible to distinguish between the thresholds corresponding to the opening of the $J=3/2$ and $J=5/2$ channels (the fine-structure splitting is smaller than the laser bandwidth).

The relative strength of the $1s3s\ ^3S$ photodetachment channel can be estimated from the number of positive ions produced when both the detachment and the excitation processes are saturated. With 1 nA of He^- approximately one ion was recorded per laser shot at 0.05 nm after the threshold. Taking the correction for the detection efficiency into account, this corresponds to that 0.2% of the detached ions are formed in the $1s3s\ ^3S$ state.

The background signal, as can be seen below threshold, is attributed primarily to collisions with rest-gas particles. Previously it was shown by Kudryavtsev and Petrunin [21] that the collisional noise observed when performing resonant-ionization spectroscopy on fast beams is dominated by the collisional excitation to a Rydberg level in the field-free interaction region and by the collisional ionization in the field of the field ionizer. In the present experiment, He Rydberg atoms are formed in the field-free interaction region, either by collisional detachment of He^- directly to the Rydberg level or by laser detachment to a lower-lying He level, followed by collisional excitation to the He Rydberg level. In the region of the field ionizer, there will be a contribution from He^+ ions formed either as a result of collisional ionization of He atoms formed by laser photodetachment or direct double-collisional detachment of He^-. In the case of saturated photodetachment the latter contribution is negligible.

The reproducibility of the position of the thresholds was checked carefully by recording several scans with the laser beam either co- or counterpropagating the ion beam. The position of the threshold can vary if the velocity of the ions is different in different scans as a result of a slightly fluctuating acceleration voltage. The maximum deviation from the average position was less than the bandwidth of the laser. The reproducibility of the laser is very good, less than 0.0005 nm, as directly observed from the excitation lines in the optogalvanic lamp and the fringe pattern of the interferometers.

The partial cross section σ_J at the opening of a new detachment channel is, according to Wigner [22], given as $\sigma_J \propto k^{l+1/2}$, where $k=\sqrt{2(\hbar\omega-\hbar\omega_J)}$ is the momentum of the outgoing electron in atomic units given by the energy difference between the photon energy $\hbar\omega$ and the threshold energy $\hbar\omega_J$. However, if the dipole polarizability α of the atomic final state is large then it is necessary to take the residual induced-dipole point-charge interaction into account, and in this case the partial photodetachment cross section is, according to O'Malley [23], given by

$$\sigma_J(k)\propto k^{l+1/2}\left(1+\frac{4\alpha k\ \ln(k)}{(2l+3)(2l+1)(2l-1)}+O(k^2)\right). \tag{3.1}$$

The dipole polarizability of the He $1s3s\ ^3S$ state was calculated to be 7903.6 a.u. For detachment to He $1s3s\ ^3S$, the angular momentum l of the outgoing electron can, according to parity and angular momentum conservation, be either 0 or 2, corresponding to either an ϵs or ϵd wave. However, close to threshold, the ϵs cross section will dominate over the ϵd wave cross section.

The data for each of the two thresholds (co- and counterpropagating) obtained in 20 scans were added and fitted with a function $[\Phi_{\mathrm{signal}}(\lambda)]$, which is essentially one Wigner threshold [Eq. (3.1)] for each of the three fine-structure levels and takes the finite width of the dye laser into account:

$$\Phi_{\mathrm{signal}}(\lambda)=\int_0^\infty \sigma(\lambda')e^{-(1/\lambda-1/\lambda')^2/\Gamma^2_{\mathrm{laser}}}\,d\left(\frac{1}{\lambda'}\right), \tag{3.2}$$

where

$$\sigma(\lambda')=\frac{\sigma_0}{\sqrt{n(\lambda')}}\left(\sum_{J=1/2}^{5/2}(2J+1)\sigma_J[k(\lambda')]\right)+\sigma_{\mathrm{background}}. \tag{3.3}$$

It is assumed that the strength of the individual channels follows the statistical weight of the initial level. $n(\lambda')$ is the

refractive index, which is assumed constant, $\sigma_{\text{background}}$ and σ_0 are fitting parameters, λ is the laser wavelength in air, and λ_J the wavelength in air at which the corresponding channel opens. The fitting parameters λ_J are restricted since the fine-structure splittings are known very accurately from previous experiments [13]. The width of the laser Γ_{laser} is estimated from the fringe pattern of the interferometers. The integral over the variable $(1/\lambda')$ in the fitting function was performed numerically.

The wavelength for the co- and counterpropagating laser ion beams $\lambda_{5/2}^{\text{co}}=414.4797$ nm and $\lambda_{5/2}^{\text{counter}}=418.4191$ nm obtained from the fitting procedure can then be converted into vacuum wavelengths, using $n(\lambda^{\text{counter}})=1.000\,281\,8$ and $n(\lambda^{\text{co}})=1.000\,282\,0$ [24,25]. The threshold energy $\hbar\omega=1/\lambda_{\text{vac}}$ corrected for the Doppler shift to all orders is obtained as the geometric means of the two measurements

$$\hbar\omega=\sqrt{\hbar\omega_{5/2}^{\text{co}}\hbar\omega_{5/2}^{\text{counter}}}=24006.02\pm0.05\ \text{cm}^{-1}. \quad (3.4)$$

The electron affinity of He $1s2s\ ^3S$ is then determined by subtracting 23 380.817 cm^{-1} from the threshold energy corresponding to the energy difference between He $1s3s\ ^3S$ and $1s2s\ ^3S$ [26]. For conversion to eV, we use the recommended factor (1 eV $=8065.5410\pm0.0024\ \text{cm}^{-1}$) [27] and obtain an electron affinity of 77.516 ± 0.006 meV.

IV. THEORY

In this work, like Bunge and Bunge [16], we will use the CI wave function to calculate the $1s2s2p\ ^4P^o$ energy. We have used a 842-term wave function (Ψ_b) to calculate the energy upper bound. Due to a better optimization, we obtained $-2\,178\,073.33\times10^{-6}$ a.u., which is 2.0×10^{-6} a.u. lower than the result obtained by Bunge and Bunge [16], but it is higher than the most recent result of Bylicki and Pestka [28], who use correlated wave functions. Using this Ψ_b, we have carried out a restricted-variation (RV) calculation for each set of the angular components. The total contribution of the RV calculation is 3.86×10^{-6} a.u. The energy convergence and the result for this RV calculation ΔE_{RV} are given in Table I.

In the restricted-variation calculation, the wave function is given by

$$\Psi=C_b\Psi_b+\sum_i C_i\Phi_i, \quad (4.1)$$

where Ψ_b is the 842-term wave function obtained earlier. It is used as a single term in Eq. (4.1). Φ_i are basis functions with new nonlinear parameters. They are optimized in a new energy calculation. The advantage of the restricted variation method is that we can saturate the functional space but avoid the numerical instability caused by linear dependence between Ψ_b and Φ_i. The disadvantage is that the method does not allow a full interaction between Ψ_b and Φ_i. The error caused by this effect depends on the size of the energy improvement ΔE_{RV}, and the error is usually more than 5% but less than 20%. Hence we need to add an extrapolation energy

TABLE I. Energy convergence of the 842-term He^- $1s2s2p\ ^4P^o$ wave function and contributions from restricted variation calculation (in $\times10^{-6}$ a.u., N is the number of terms in Ψ_b).

Angular components ($l_1l_2l_3$)	N	ΔE_b	ΔE_{RV}
001	188	2 173 887.60	0.770
012	179	3480.45	0.584
023	86	43.85	0.319
034	30	6.13	0.383
045	20	1.38	0.182
056	10	0.32	0.170
067	10	0.12	0.071
078	10	0.05	0.034
089	10	0.02	0.018
111	85	519.19	0.217
113	13	2.96	0.049
124	4	0.10	0.039
135			0.017
221	104	52.33	0.307
331	22	4.68	0.214
441	7	0.90	0.184
551	7	0.25	0.076
661	7	0.08	0.034
771	7	0.03	0.017
881			0.023
223	35	0.82	0.054
234	4	0.06	0.066
245	4	0.01	0.017
256			0.010
Total	842	2 178 073.33	3.86

of $(0.50\pm0.30)\times10^{-6}$ a.u. over the computed 3.86×10^{-6} a.u. to the total energy. In addition, the higher angular components not included in Table I will also make a contribution. By studying the convergence pattern, these contributions can be extrapolated. The neglected higher angular momentum contribution is about $(0.16\pm0.02)\times10^{-6}$ a.u. Adding the results from the upper bound RV calculation and extrapolation, we obtain $(-2\,178\,077.85\pm0.32)\times10^{-6}$ a.u. for the total nonrelativistic energy. This energy agrees with the result of Bylicki and Pestka [28]. The uncertainty, 0.32×10^{-6} a.u., is smaller than that of Bunge and Bunge [16] by about 0.8×10^{-6} a.u. Compared to the accurate He $1s2s\ ^3S$ energy, $-2\,175\,229.38\times10^{-6}$ a.u. [29], the nonrelativistic part of the electron affinity is 2848.47×10^{-6} a.u.

To determine the relativistic correction to the energy, we calculate the mass polarization, the relativistic correction to the kinetic energy (P^4), the Darwin term, the orbit-orbit, spin-orbit, spin-spin, and spin-other-orbit interactions. The mass-polarization effect is calculated to infinite order, whereas the other interactions are calculated with first-order perturbation theory. The helium atomic mass used is 4.002 603 24 amu given by Wapstra and Audi [30]. The results of this calculation are given in Table II. In 1984, Chung [31] calculated the relativistic correlations for He^- $1s2s2p\ ^4P^o$, using a 92-term CI function. Compared

TABLE II. Energy and relativistic corrections for He^- $1s2s2p\ ^4P^o$ and electron affinity of He $1s2s\ ^3S$ (in 10^{-6} a.u.).

	He^- $1s2s2p\ ^4P^o_{5/2}$	He $1s2s\ ^3S$	Electron affinity
Nonrelativistic energy			
842-term wave function	−2 178 073.33		
ΔE_{RV}	−3.86		
higher angular comp.	−0.16(2)		
extrapolation	−0.50(30)		
Total nonrelativistic energy	−2 178 077.85(32)	−2 175 229.38	2848.47(32)
Relativistic correction			
P^4 and Darwin	−112.356	−115.074	
orbit-orbit	0.515	−0.087	
mass polarization	−2.618	1.019	
spin-orbit	0.5131		
spin-spin	0.0932		
spin-other-orbit	−0.8690		
Total correction	−114.72	−114.14	0.58(3)
QED correction			0.09(7)
Total affinity			2849.14(42)
Affinity (meV)			
Theory (this work)			77.518(11) meV
Experiment (this work)			77.516(6) meV
Theory (Refs. [16,28])			77.51(4)
Experiment (Ref. [15])			77.67(12) meV

with the 842-term wave function used in this work, the results for the mass polarization and orbit-orbit interaction remain the same to the digit quoted, but the results of the P^4 and the Darwin term are reduced by about 0.2×10^{-6} a.u., and the shift of the $J=5/2$ from the center of gravity is reduced by about 0.01×10^{-6} a.u. The splittings of the fine structure in this calculation are much improved and yield $\Delta E_{1/2-3/2}=0.2621\ \mathrm{cm}^{-1}$ and $\Delta E_{3/2-5/2}=0.0279\ \mathrm{cm}^{-1}$. These values are in agreement with the precision experiment [13] to within 0.26% and 1.3%, respectively.

To estimate the contribution of the relativistic perturbation to electron affinity, we calculate its correction to the energy of He $1s2s\ ^3S$ by using a 288-term CI wave function. The upper bound for this wave function is −2.175 229 13 a.u., very close to the exact value [29]. If we subtract the relativistic correction of He $1s2s\ ^3S$ from that of the He^- $1s2s2p\ ^4P^o$, we obtain 0.58×10^{-6} a.u. To account for possible errors in the relativistic correction and higher-order effects, we assign an uncertainty of 0.03×10^{-6} a.u.

The QED contribution to the ionization potential of the $2p$ electron in He $1s2p\ ^3P$ is 0.19×10^{-6} a.u. [17]. In He^- $1s2s2p\ ^4P^o$, this contribution is expected to be somewhat smaller due to the presence of the $2s$ electron. The contribution will probably fall in the range of $(0.09\pm0.07)\times10^{-6}$ a.u. Hence we assume the contribution of QED to the affinity to be $(0.09\pm0.07)\times10^{-6}$ a.u. Adding the contribution from the nonrelativistic energy, relativistic correction, and QED effects, we find the theoretical total electron affinity of He $1s2s\ ^3S$ to be $(2849.14\pm0.42)\times10^{-6}$ a.u. Using 1 a.u. $=27.207\ 67$ eV, this corresponds to 77.518 ± 0.011 meV.

V. CONCLUSION

In summary, the presented experimental and theoretical values 77.516 ± 0.006 meV and 77.518 ± 0.011 meV are in good agreement with each other and with the remarkably accurate prediction, 77.51 ± 0.04 meV, of Bunge and Bunge [16] and recently Bylicki and Prestka [28]. They are, however, in slight disagreement with the value 77.67 ± 0.12 meV obtained in the previous experimental work of Walter *et al.* [15]. With the remarkable success *ab initio* calculations have had in predicting the EA of the lighter atoms (H, He, Li, and Be), it seems tempting to test whether the theory also can predict accurate values for the EA of boron, the next element in the Periodic Table. The best experimental value available for the EA of boron, 277 ± 10 meV [32], is, however, not sufficiently accurate to match the accuracy of a recent theoretical multiconfiguration Hartree-Fock calculation, yielding 279.5 ± 2.0 meV [33]. We are currently investigating the possibility of measuring the affinity of boron with an accuracy capable of matching the theoretical value.

ACKNOWLEDGMENTS

The experimental work is part of the research program of the ACAP center, which is funded by the Danish National Research Foundation. The theoretical work is supported by the National Science Foundation Grant No. PHY 93-14907.

[1] K. R. Lykke, K. K. Murray, and W. C. Lineberger, Phys. Rev. A **43**, 6104 (1991).
[2] D. M. Neumark, K. R. Lykke, T. Andersen, and W. C. Lineberger, Phys. Rev. A **32**, 1890 (1985).
[3] G. Haeffler *et al.*, Phys. Rev. A **53**, 4127 (1996).
[4] P. Kristensen, V. V. Petrunin, H. H. Andersen, and T. Andersen, Phys. Rev. A **52**, R2508 (1995).
[5] H. H. Andersen, P. Balling, V. V. Petrunin, and T. Andersen, J. Phys. B **29**, L415 (1996).
[6] C. L. Pekeris, Phys. Rev. **112**, 1649 (1958).
[7] C. L. Pekeris, Phys. Rev. **126**, 1470 (1962).
[8] K. Aashamar, Nucl. Instrum. Methods **90**, 263 (1970).
[9] J.-J. Hsu and K. T. Chung, Phys. Rev. A **52**, R898 (1995).
[10] T. Andersen *et al.*, Phys. Rev. A **47**, 890 (1993).
[11] R. Novick and D. Weinflash, in *Proceedings of the International Conference on Precision and Fundamental Constants*, Natl. Bur. Stand. (U.S.) Spec. Publ. No. 343, edited by D. N. Langenberg and N. N. Baylor (U.S. GPO, Washington, DC, 1970), p. 403.
[12] T. Brage and C. F. Fischer, Phys. Rev. A **44**, 72 (1991).
[13] D. L. Mader and R. Novick, Phys. Rev. Lett. **29**, 199 (1972).
[14] J. R. Peterson, Y. K. Bae, and D. L. Huestis, Phys. Rev. Lett. **55**, 692 (1985).
[15] C. W. Walter, J. A. Seifert, and J. R. Peterson, Phys. Rev. A **50**, 2257 (1994).
[16] A. V. Bunge and C. F. Bunge, Phys. Rev. A **30**, 2179 (1984).
[17] G. W. F. Drake, Can. J. Phys. **66**, 586 (1988).
[18] K. T. Chung and X. W. Zhu, Phys. Scr. **48**, 292 (1993).
[19] Yu. A. Kudryavtsev and V. V. Petrunin, Zh. Éksp. Teor. Fiz. **94**, 76 (1988) [Sov. Phys. JETP **67**, 691 (1988)].
[20] V. Kaufman and B. Edlén, J. Phys. Chem. Ref. Data **3**, 825 (1974).
[21] Yu. A. Kudryavtsev and V. V. Petrunin, Zh. Éksp. Teor. Fiz. **99**, 81 (1991) [Sov. Phys. JETP **72**, 43 (1991)].
[22] E. P. Wigner, Phys. Rev. **73**, 1002 (1948).
[23] T. F. O'Malley, Phys. Rev. **137**, A1668 (1965).
[24] B. Edlén, J. Opt. Soc. Am. **43**, 339 (1953).
[25] B. Edlén, Metrologia **2**, 71 (1966).
[26] G. W. F. Drake, in *Atomic, Molecular and Optical Physics Handbook* (AIP, New York, 1996), Chap. 11.
[27] E. R. Cohen and B. N. Taylor, J. Phys. Chem. Ref. Data **17**, 1795 (1988).
[28] M. Bylicki and G. Pestka, J. Phys. B **29**, L353 (1996).
[29] Y. Accad, C. L. Pekeris, and B. Schiff, Phys. Rev. A **4**, 516 (1971).
[30] A. H. Wapstra and G. Audi, Nucl. Phys. A **432**, 1 (1985).
[31] K. T. Chung, Phys. Rev. A **29**, 439 (1984).
[32] C. S. Feigerle, R. R. Cordermann, and W. C. Lineberger, J. Chem. Phys. **74**, 1513 (1981).
[33] C. F. Fischer, A. Ynnerman, and G. Gaigalas, Phys. Rev. A **51**, 4611 (1995).